

See discussions, stats, and author profiles for this publication at: <https://www.researchgate.net/publication/271545759>

The 3-DoF bicycle model with the simplified piecewise linear tire model

Conference Paper · December 2013

DOI: 10.1109/MEC.2013.6885617

CITATIONS

16

READS

14,825

4 authors:



Gang Liu

6 PUBLICATIONS 83 CITATIONS

SEE PROFILE



Hongbin Ren

Beijing Institute of Technology

33 PUBLICATIONS 605 CITATIONS

SEE PROFILE



Sizhong Chen

Beijing Institute of Technology

43 PUBLICATIONS 863 CITATIONS

SEE PROFILE



Wang Wenzhu

Jilin University

2 PUBLICATIONS 17 CITATIONS

SEE PROFILE



Development of Effective Bicycle Model for Wide Ranges of Vehicle Operations

2014-01-0841
Published 04/01/2014

Hongbin Ren

Beijing Institute of Technology

Taehyun Shim

Univ. of Michigan

Jemyoung Ryu

Hyundai Motor Co.

Sizhong Chen

Beijing Institute of Technology

CITATION: Ren, H., Shim, T., Ryu, J., and Chen, S., "Development of Effective Bicycle Model for Wide Ranges of Vehicle Operations," SAE Technical Paper 2014-01-0841, 2014, doi:10.4271/2014-01-0841.

Copyright © 2014 SAE International

Abstract

This paper proposes an effective nonlinear bicycle model including longitudinal, lateral, and yaw motions of a vehicle. This bicycle model uses a simplified piece-wise linear tire model and tire force tuning algorithm to produce closely matching vehicle trajectory compared to real vehicle for wide vehicle operation ranges. A simplified piece-wise tire model that well represents nonlinear tire forces was developed. The key parameters of this model can be chosen from measured tire forces. For the effects of dynamic load transfer due to sharp vehicle maneuvers, a tire force tuning algorithm that dynamically adjusts tire forces of the bicycle model based on measured vehicle lateral acceleration is proposed. Responses of the proposed bicycle model have been compared with commercial vehicle dynamics model (CarSim) through simulation in various vehicle maneuvers (ramp steer, sine-with-dwell). The simulation results show that the trajectory of the proposed bicycle model is well matched with the CarSim vehicle model for ramp steer and sine-with-dwell maneuvers at various vehicle operating conditions. This model can be a useful tool for the development of effective vehicle chassis control systems.

Keywords

Bicycle model, reference model, vehicle dynamics, piece-wise linear tire model

Introduction

In the design of an effective control system, it is important to have a system model that is relatively simple and well reflects the behavior of the real systems. Many different vehicle models with various complexities have been proposed and used in various vehicle chassis control systems [1, 2, 3]. In general, model accuracy is closely related to model complexity. Due to the computational burden in the control system, it is difficult to use a complex model in the control system. For this reason, various assumptions have been used in the model to reduce the complexity while maintaining the accuracy related to the control objectives.

Bicycle models have been widely used in various vehicle control systems such as yaw stability control, sideslip control, and trajectory control, etc. In these control systems, a linear bicycle model or a linearized bicycle model for vehicle operating conditions are often used and generate desired (reference) vehicle responses needed for the control systems. When vehicle runs under normal driving conditions, a bicycle model can well represent real vehicle behaviors. When a vehicle runs severe maneuvers that produce large lateral accelerations, it is difficult to track real vehicle responses using a bicycle model due to the effects of nonlinear tire forces and dynamic load transfer associated vehicle dynamics. For this reason, the use of bicycle model is limited. It is desirable to have a bicycle model that can closely represent real vehicle behavior for wide vehicle operation ranges.

An accurate and simple model is essential for the design of an effective controller and state estimator. In an effort to improve the accuracy of bicycle models, several approaches have been proposed. Naima [1] proposed a fuzzy logical feedback to tune the front and rear stiffness value to cope the behavior of the lateral tire forces including the linear, decreasing and saturated regions. Chen [2] investigated the bicycle dynamic properties by using system identification approaches. C. Westermarck [3] optimized the tire stiffness parameters in the bicycle model, the results revealed that this method is better compliance on high friction road than on the low friction road, an explanation to this is that the model does not consider friction and that the tire forces in the bicycle model are linear functions of the slip angles, so linear tire in the bicycle model makes it only valid for driving on high friction or low speed where no sliding occurs [4].

This paper compares vehicle responses of three different bicycle models: a bicycle model with a linear tire, a bicycle model with a simplified tire model, and a bicycle model with a simplified tire model along with a parameter tuning algorithm. This tuning algorithm uses measured sensor information (lateral acceleration) to correct the model errors.

This paper is organized as follows. First, the linear bicycle model and nonlinear bicycle model are introduced; second, the simplified tire model is proposed, and the comparison results are presented; and the tuning method is proposed and the simulation and comparison are provided. At last, summary and conclusion are given.

Bicycle Model

The bicycle model has a long history in automobile steering and stability studies, as well as vehicle active safety control [5, 6, 7], because of the simple structure and computational efficiency. Fig. 1 shows a typical bicycle model used in the literature [8, 9, 10]. This model is based on the following set of assumptions: at front and rear axles, the left and right wheels are lumped in a single wheel; heave, roll and pitch motions are ignored (no load transfer due to roll and pitch motions).

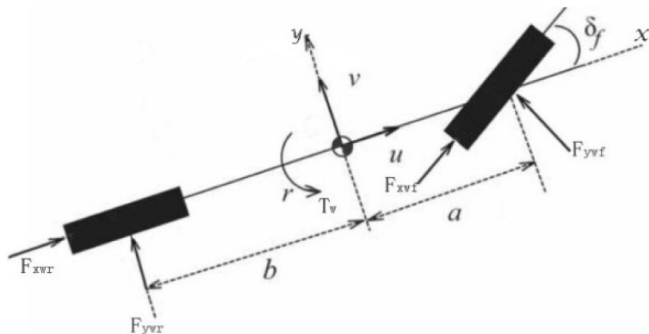


Fig. 1. Schematic of bicycle model

Linear Bicycle Model

Eq. (1) shows a linear bicycle model of the vehicle with two degree of freedom (DoF) that is widely used in the literature. This model only considers vehicle lateral motion (y), and yaw motion (r). It is assumed that the load shift is due to vehicle

lateral dynamics is negligible and vehicle runs on a smooth road with a constant speed. In addition, this model assumes a linear lateral tire force characteristics with respect to tire slip angle.

$$\begin{bmatrix} \dot{v} \\ \dot{r} \end{bmatrix} = \begin{bmatrix} -\frac{C_f + C_r}{mu} & -u - \frac{aC_f - bC_r}{mu} \\ -\frac{aC_f - bC_r}{I_z u} & -\frac{a^2 C_f + b^2 C_r}{I_z u} \end{bmatrix} \begin{bmatrix} v \\ r \end{bmatrix} + \begin{bmatrix} \frac{C_f}{m} \\ \frac{aC_f}{I_z} \end{bmatrix} \delta_f \quad (1)$$

In the above equation, δ_f is the road wheel input; C_f , C_r are the front and rear tire cornering stiffness, respectively; u is the vehicle speed.

There are some limitations in the applications of a linear bicycle model for design of control systems and state estimation algorithm. The tire lateral force characteristics to slip angle can be approximated as a linear relationship when a vehicle lateral maneuver involves in a less than 0.3 g lateral acceleration. Since the linear bicycle mode uses a linear tire force characteristics, it is fairly accurate when the lateral tire force generation falls into the linear range. As a vehicle slip angle increases due to a large steering maneuvers that results in large lateral acceleration, the predicted vehicle responses from the linear bicycle model are significantly different compared to those of actual vehicle. This is due to the nonlinear relationship between the tire lateral force and tire slip angle.

In order to have an effective bicycle model for vehicle operating with large lateral acceleration, it is necessary to use a tire model that can reflect the nonlinear behavior tire.

Nonlinear Bicycle Model

In this section, a nonlinear bicycle model which considers the longitudinal (X), lateral (Y), and yaw motion (Ψ) is presented. For this model, it is assumed that the mass of a vehicle is entirely in the rigid base of a vehicle, and it considers the pitch load transfers while neglecting the lateral load transfer caused by roll motion. The nonlinear bicycle dynamic equations can be described as:

$$m(\dot{u} - vr) = \sum F_{xi} \quad (i = f, r) \quad (2a)$$

$$(\dot{v} + ur) = \sum F_{yi} \quad (i = f, r) \quad (2b)$$

$$I_z \dot{r} = F_{yf} \cdot a - F_{yr} \cdot b \quad (2c)$$

$$r = \dot{\psi} \quad (2d)$$

Where, F_{xi} , F_{yi} are longitudinal and lateral tire forces along x , y -axis, respectively. These forces can be computed by the longitudinal tire force (F_{wxi}), lateral force (F_{wyi}) and the wheel steer angle (δ_i) as:

$$\begin{cases} F_{xi} = F_{xwi} \cos \delta_i - F_{ywi} \sin \delta_i \\ F_{yi} = F_{xwi} \sin \delta_i + F_{ywi} \cos \delta_i \end{cases} \quad (i = f, r) \quad (3)$$

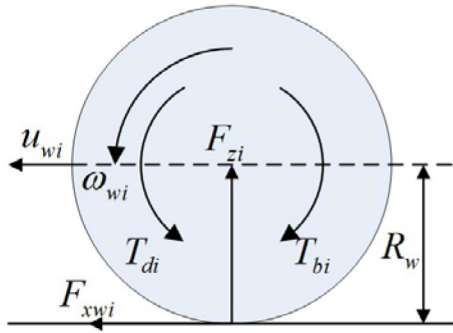


Fig. 2. Dynamic model of a wheel

With application of driving torque T_d and braking torque T_b on each wheel, which is shown in Fig. 2, the rotational motion can be derived as:

$$I_z \dot{\omega}_{wi} = T_{di} - F_{xi} R_w - T_{bi} \quad (i = f, r) \quad (4)$$

Table 1. Vehicle Parameters

Sprung mass	m_s	1111kg
Front unsprung mass	m_{uf}	60kg
Rear unsprung mass	m_{ur}	60kg
Yaw moment of inertia	I_z	2031kgm ²
c.g. distance to front wheels	a	1.04m
c.g. distance to rear wheels	b	1.56m
The radius of the wheel	R_w	0.28m

The trajectory of vehicle center of gravity in an absolute inertial coordination can be determined by,

$$\begin{cases} \dot{X} = u \cos \psi - v \sin \psi \\ \dot{Y} = u \sin \psi + v \cos \psi \end{cases} \quad (5)$$

Tire Model

The performance of a vehicle heavily depends on the tire forces which are generated in the tire road patches. Thus, in the simulation of the vehicle dynamic response, the accuracy of a simulation results strongly relies on the correctness of the longitudinal and lateral tire forces calculated by the tire model. There are many different tire models used in vehicle simulation study such as 'Magic Formula' [11], 'Doguff tire model' [12], 'Gim tire model' [13], and 'Uni-tire' [14].

These tire models typically require tire lateral slip angle, longitudinal slip, vertical force, camber angle, and tire-road friction as inputs, and generate lateral tire force, and longitudinal

tire force as outputs into the vehicle dynamics model. Assuming the small lateral velocity and yaw angular velocity, the following equations are used for the lateral slip angle:

$$\alpha_f = \delta_f - \frac{v + a \cdot r}{u_{wf}} \quad \alpha_r = \frac{b \cdot r - v}{u_{wr}} \quad (6)$$

The tire longitudinal slip ratio for each individual tire is given by:

$$\begin{cases} s_{wi} = 1 - \frac{u_{wi}}{R_w \omega_{wi}}, & u_{wi} \leq R_w \omega_{wi}, \\ s_{wi} = \frac{R_w \omega_{wi}}{u_{wi}} - 1, & u_{wi} > R_w \omega_{wi}. \end{cases} \quad (7)$$

The tire longitudinal speed required in the calculation of longitudinal slip and lateral slip angle can be determined as:

$$\begin{cases} u_{wf} = u \cos \delta_i + (v + ar) \sin \delta_i \\ u_{wr} = u \cos \delta_i + (v - br) \sin \delta_i \end{cases} \quad (i = f, r) \quad (8)$$

With only considering pitch load transfer, and ignoring the roll load transfer, the vertical forces F_z of the front and rear tires are calculated by:

$$\begin{cases} F_{zf} = \frac{m_s g b}{L} + m_{uf} g - \Delta F_{zf} \\ F_{zr} = \frac{m_s g a}{L} + m_{ur} g + \Delta F_{zr} \end{cases} \quad (9)$$

Where ΔF_{zf} and ΔF_{zr} are the vertical loads transfer caused by pitch motion of the body:

$$\begin{cases} \Delta F_{zf} = \frac{(\dot{u} - vr)(m_s h_{cg} + m_{uf} h_{uf})}{L} \\ \Delta F_{zr} = \frac{(\dot{u} - vr)(m_s h_{cg} + m_{ur} h_{ur})}{L} \end{cases} \quad (10)$$

Magic Formula Tire

The Magic formula tire model is one of the most widely used tire models in the simulation of vehicle dynamics. This tire model is an empirical model that fits well with measured tire test data and it can handle the interaction between the tractive force and the cornering force in combined braking and steering condition. Although this approach yields realistic tire behavior, it requires many experimental coefficients needed in the model. The longitudinal and cornering forces can be calculated using the normal force (F_z), slip angle (α), tire road friction coefficient (μ), and longitudinal slip ratio (s):

$$[F_{xwi}, F_{ywi}] = MF(F_{zi}, \alpha_i, s_i, \mu) \quad (i = f, r) \quad (11)$$

Piece-Wise Linear Tire

Although the Magic Formula tire model well describes the realistic tire behaviors, it requires many experimental tire coefficients. It is often desirable to use an analytical tire model [12, 13] that requires relatively small physical parameter in vehicle dynamics simulation and vehicle control system development.

The linear tire model has been widely used in many vehicle applications [14]. This model is effective in the simulation of normal driving conditions where tire slip and slip angle are small. Since vehicle operates in this region, the longitudinal and lateral tire force generations are close to linear in terms of tire slip and slip angle. However, as vehicle maneuvers at severe conditions, the tire slip and slip angle become large and the tire force generations has nonlinear behavior. In this condition, the linear tire model can't properly represent realistic tire behaviors. For this reason, a simplified piecewise tire model has been used. It closely matches with the Magic Formula tire model for the wide ranges of vehicle operations. The following shows the longitudinal and lateral tire forces in the simplified piecewise tire model.

The pure longitudinal tire force is determined as:

$$F_x = \begin{cases} C_x \cdot s & |s| < s_1 \\ C_x \cdot s_1 \cdot \text{sgn}(s_1) & s_1 \leq |s| < s_2 \\ \left(C_x \cdot s_1 - \frac{C_x \cdot s_1 - F_{end}}{s_2 - 1} \cdot (|s| - s_2) \right) \cdot \text{sgn}(s_1) & |s| > s_2 \end{cases} \quad (12)$$

$$\begin{aligned} \text{Here, } s_1 &= 7s_{1_nom}; C_x = C_{x_nom} \left(1 + \frac{F_z - F_{z_nom}}{F_{z_nom}} \right); \\ s_2 &= s_{2_nom} \left(1 + \frac{F_z - F_{z_nom}}{6F_{z_nom}} \right) - 2; F_{end} = \left(\frac{F_{end_nom}}{F_{z_nom}} + \frac{F_z - F_{z_nom}}{4F_{z_nom}} \right) 0.8 \mu F_z; \\ F_{end_nom} &= 3000 \left(1 + \frac{F_z - F_{z_nom}}{6F_{z_nom}} \right). \end{aligned}$$

For the pure lateral tire force is:

$$F_y = \begin{cases} -C_y \cdot \alpha & |\alpha| < 0.85\alpha_0 \\ -\frac{C_y}{6} \cdot (|\alpha| + 4.25\alpha_0) \cdot \text{sgn}(\alpha) & 0.85\alpha_0 \leq |\alpha| < 1.75\alpha_0 \\ F_{peak} \cdot \text{sgn}(\alpha) & |\alpha| > 1.75\alpha_0 \end{cases} \quad (13)$$

$$\begin{aligned} \text{Here, } C_y &= C_{y_nom} \left(1 + \frac{F_z}{F_{z_nom}} \right) / 2.5; \alpha_0 = \frac{F_{peak}}{C_y}; \\ F_{peak} &= (0.9 - 0.182 \left(\frac{F_z}{F_{z_nom}} - 1 \right))^{0.5}. \end{aligned}$$

For the longitudinal and lateral tire forces in the combined driving and steering condition, the following function [15] has been used:

$$\sigma_x = -\frac{s}{s+1} \quad \sigma_x^* = \frac{\sigma_x}{\sigma_{x_max}} \quad (14)$$

$$\sigma_y = \frac{\tan(\alpha)}{s+1} \quad \sigma_y^* = \frac{\sigma_y}{\sigma_{y_max}} \quad (15)$$

$$\sigma_{total} = \sqrt{\sigma_x^2 + \sigma_y^2} \quad \sigma_{total}^* = \sqrt{\sigma_x^{*2} + \sigma_y^{*2}} \quad (16)$$

$$s' = \frac{\sigma_{total}^* \cdot \sigma_{x_max} \cdot \text{sign}(\sigma_x)}{1 + \sigma_{total}^* \cdot \sigma_{x_max} \cdot \text{sign}(\sigma_x)} \cdot \frac{\mu_0}{\mu} \quad (17)$$

$$\alpha' = \arctan(\sigma_{total}^* \cdot \sigma_{y_max} \cdot \text{sign}(\sigma_y)) \cdot \frac{\mu_0}{\mu} \quad (18)$$

$$F_x = F_x(s', F_z) \cdot \mu \cdot \frac{\sigma_x}{\sigma_{total}} \cdot \text{sign}(s') \quad (19)$$

$$F_y = F_y(\alpha', F_z) \cdot \mu \cdot \frac{\sigma_y}{\sigma_{total}} \cdot \text{sign}(\alpha') \quad (20)$$

Table 2. Piece-wise Linear Tire Model Parameters

Nominal load	N_o	4000N
Nominal slip ratio1	s_{1_nom}	0.01
Nominal slip ratio2	s_{2_nom}	0.25
Nominal longitudinal stiffness	C_{x_nom}	420000
Nominal lateral stiffness	C_{y_nom}	1000N/deg
Friction coefficient	μ_0	1

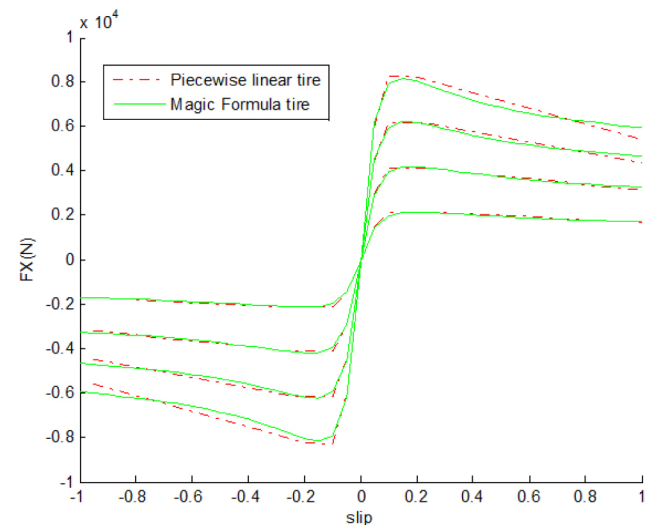


Fig.3. Comparison of tire longitudinal tire force between MF tire and piecewise linear tire for different normal forces (2000N, 4000N, 6000N and 8000N)

In order to validate the effectiveness of piece-wise linear tire model, its tire force characteristics have been compared to Magic Formula tire model. Fig. 3 compares the pure longitudinal tire forces between two models for different normal forces. The pure lateral forces are compared in Fig. 4. As shown in the figures, the tire forces of the piece-wise linear model are well matched with those of Magic Formula tire model.

Figs. 5 and 6 show the comparison of tire forces during the combined driving and steering conditions. Fig. 5 compares the longitudinal tire force with different slip angle at a normal force of 4000 N. The lateral tire forces for a different tire slip are compared in Fig. 6. As shown in the figures, the piece-wise linear tire model are well tracked the Magic Formula tire model, although there are some discrepancies in the tire forces.

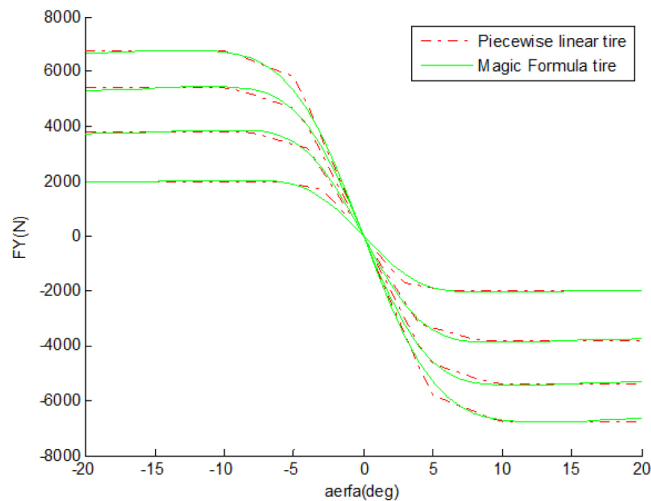


Fig.4. Comparison of lateral tire force between MF tire and piecewise linear tire for different normal forces (2000N, 4000N, 6000N and 8000N)

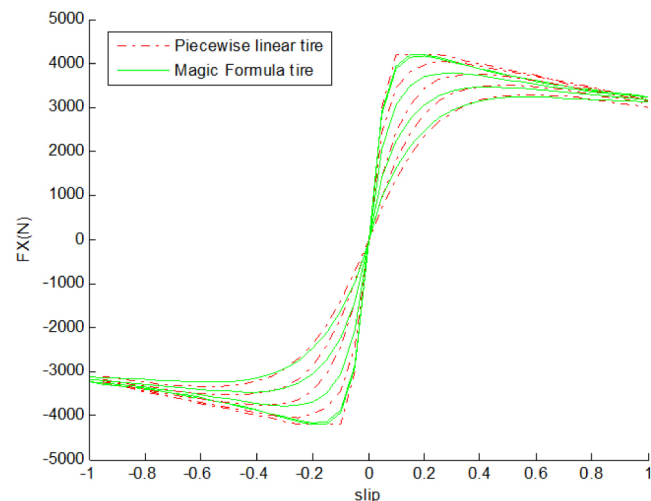


Fig.5. Comparison of longitudinal tire force between MF tire and piecewise linear tire for different slip angles (0°, 4°, 8°, 12°, 16°) ($F_z=4000\text{N}$)

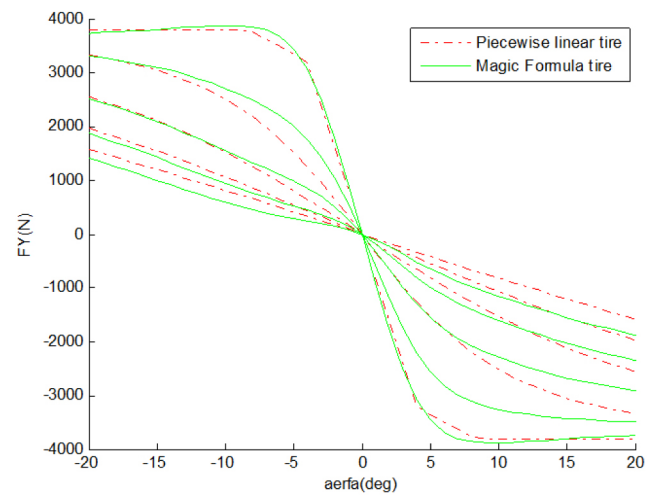


Fig.6. Comparison of lateral tire force between MF tire and piecewise linear tire for different longitudinal slips (0, 0.2, 0.4, 0.6, 0.8) ($F_z=4000\text{N}$)

Vehicle Model Comparison

In this section, vehicle responses of two different bicycle models discussed in the previous section (a linear and a nonlinear bicycle models) are compared with CarSim model. CarSim [18] is vehicle dynamics software widely used in the automotive industry. During the simulation, CarSim model is assumed to be a real vehicle. Vehicle parameters shown in Table 1 and tire parameters in Table 2 are used in the simulation. A ramp steer input shown in Fig. 7 is applied to a vehicle while a vehicle runs at a constant speed 30 km/h and 120 km/h.

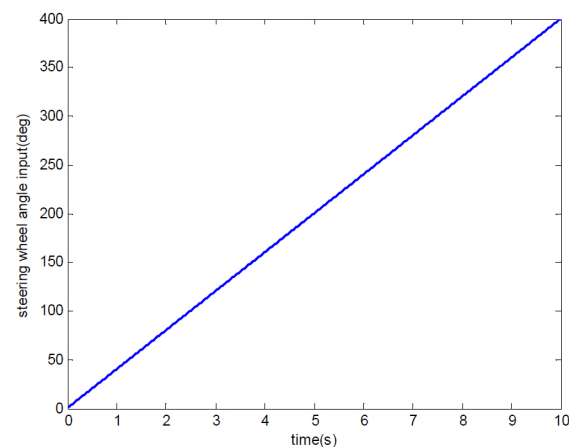


Fig.7. Steering wheel inputs for ramp steer

Fig. 8 shows comparison in vehicle trajectories of three different vehicle models at the speed of 30 km/h. When the vehicle speed is low, the trajectory of the linear bicycle model and the nonlinear bicycle model are matched very well with the CarSim results.

Fig. 9 compares vehicle trajectories with the vehicle speed of 120 km/h. The trajectory of a linear bicycle model is significantly different with others, which is expected since the linear bicycle model doesn't consider the tire force saturation. For the trajectory of a nonlinear vehicle model is better matched with that of a CarSim. However, as a steering input

increases, the nonlinear bicycle model becomes more under steer compared to CarSim and its trajectory becomes wider from CarSim vehicle trajectory.

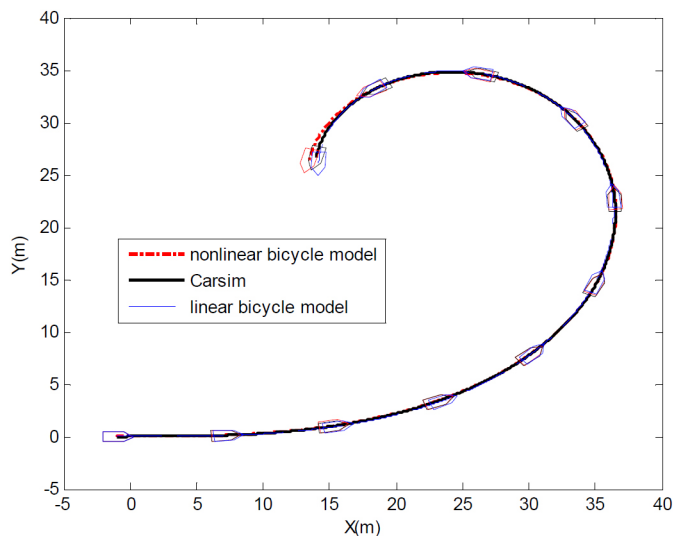


Fig.8. Vehicle trajectory comparison for the ramp steer input at a speed of 30 km/h

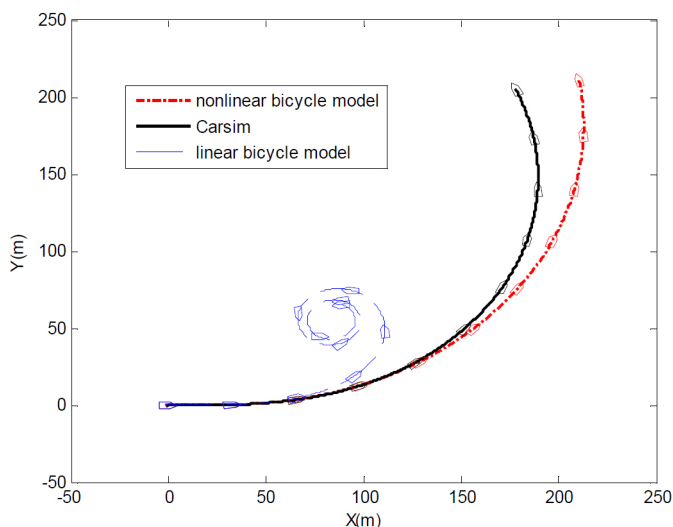


Fig.9. Vehicle trajectory comparison for the ramp steer input at a speed of 120 km/h

To further illustrate the scopes of the application of the different models, Fig. 10 compares vehicle trajectories of three vehicle models for different vehicle speeds when a ramp steer input shown in Fig. 7 is applied. As seen on Fig. 10, the trajectory of the linear bicycle model is well matched with other vehicle models at the speed of 30 km/h. As vehicle speed increases to 60 km/h, 90 km/h and 120 km/h, the trajectory of a linear bicycle model deviates first and the trajectory of nonlinear model well follows till 60 km/h. With increased steering input and vehicle speed, the tire lateral slip angle becomes bigger and vehicle experiences large lateral acceleration. When a vehicle operates in this condition, the tire lateral force becomes

saturated and is not proportionally increased with a tire lateral slip angle, and lateral vehicle load transfer becomes larger. Thus, it is critical to include these effects in the bicycle model.

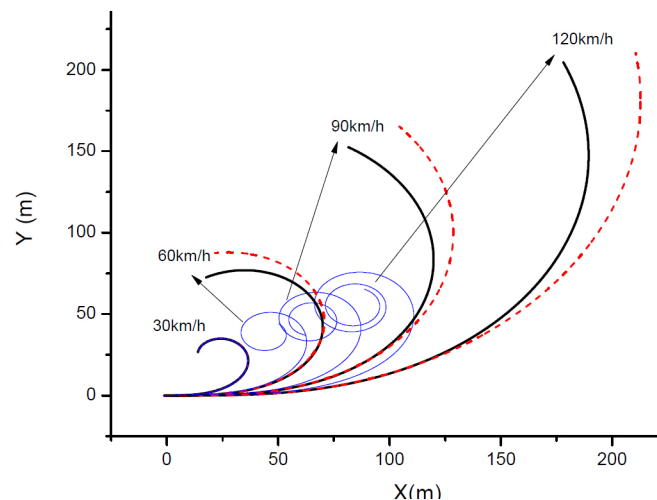


Fig.10. Vehicle trajectory comparison for different vehicle speeds: CarSim (black-thick lines); nonlinear bicycle model (dotted lines); linear bicycle model (the thin lines)

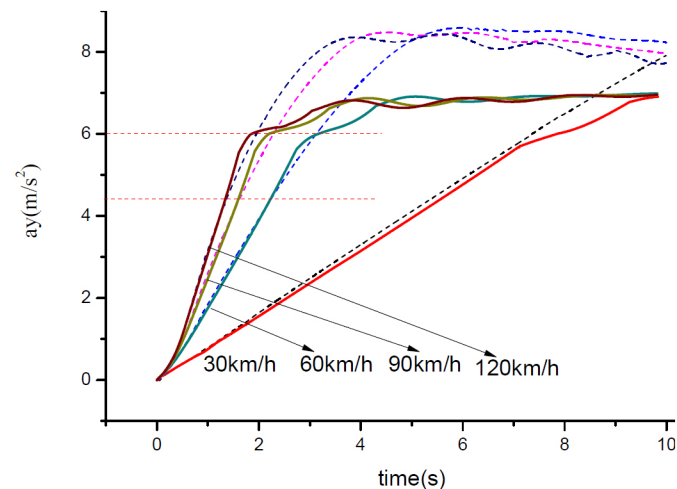


Fig. 11. Vehicle lateral acceleration comparison (dotted line-CarSim; solid line- nonlinear bicycle model)

Fig. 11 compares vehicle lateral acceleration between the nonlinear bicycle model and CarSim model for different vehicle speed when a ramp steer input is applied. The developed lateral acceleration is similar for two different models when the lateral acceleration is less than 0.45 g for all speeds. As vehicle speed increases, the developed lateral acceleration above 0.45 g is quite different between two models. In the lateral acceleration between 0.45 g and 0.6 g, the nonlinear bicycle model has bigger lateral acceleration values. For the lateral acceleration region above 0.6 g, CarSim model has a bigger lateral acceleration and the nonlinear bicycle model cannot provide sufficient tire lateral forces. Because of this, vehicle trajectories are also different as vehicle runs at higher speed.

The differences in vehicle trajectory and lateral acceleration between two models can be explained in two aspects: tire model difference and dynamic normal force variations. Since the piece-wise linear tire model introduced in the earlier section has been validated with MF tire model, the major discrepancy is coming from the incorrect use of tire normal force without considering the dynamic load transfer. The following section proposes a tuning methodology of a bicycle model that can be closely matched to CarSim model for wide vehicle operation range including large steering angle and high speed.

Bicycle Model Tuning Algorithm

In the nonlinear bicycle model, the effect of lateral load transfer is not considered. With a large steering input at a high speed, large lateral load transfer will occur during vehicle maneuver. Since the lateral tire force is strongly influenced by tire vertical force, it is crucial to have accurate tire vertical forces in the model. The differences in vehicle responses between CarSim model and nonlinear bicycle model are due to incorrect tire normal forces.

In order to incorporate accurate tire normal force in the model, the following procedures are proposed. Since a dynamic load transfer is strongly related to vehicle lateral acceleration, this method uses vehicle lateral acceleration. The load transfer ratio R is estimated from the lateral acceleration shown in Eq. (21).

$$R = \frac{\Delta F}{mg/2} = \frac{ma_y h_{cg}}{mgB/2} \quad (21)$$

Where, ΔF is the roll load transfer; a_y is the lateral acceleration; h_{cg} is the mass center height; B is the track width.

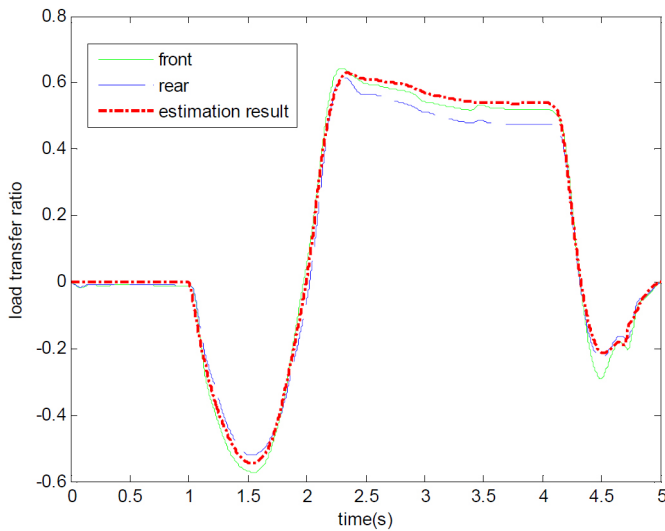


Fig. 12. Comparison of a roll load transfer between CarSim and estimated values at 120kph (front, rear-front and rear axes roll load transfer ratio in CarSim, respectively)

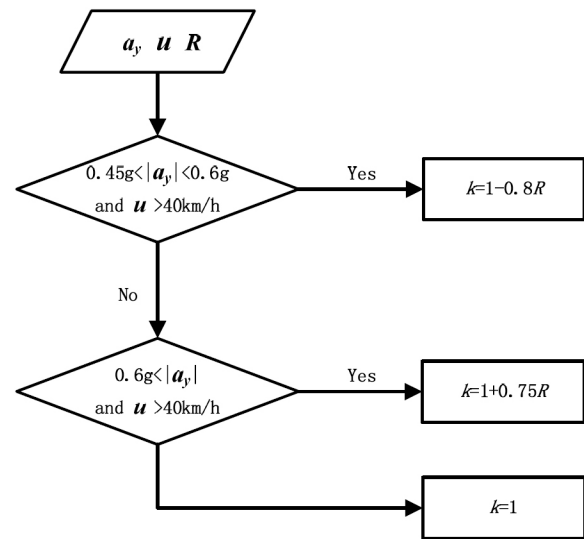


Fig. 13. A flow chart of the proposed tuning algorithm

$$\begin{cases} F_X = F_X \cdot k \\ F_Y = F_Y \cdot k \end{cases} \quad (22)$$

The proposed tuning algorithm in Fig. 13 is determined by observation of the following vehicle responses:

1. When the vehicle speed is low (less than 40 kph), the nonlinear bicycle mode is good, no tuning is required;
2. When the vehicle speed is increasing, the lateral acceleration is increasing to a certain area ($0.45 \text{ g} < a_y < 0.65 \text{ g}$), the nonlinear bicycle model is trend to oversteering, so the coefficient $k < 1$;
3. When the vehicle lateral acceleration exceeds a certain value ($> 0.65 \text{ g}$), the model tends to understeering, so the coefficient $k > 1$;
4. In the proposed tuning algorithm, the coefficient k is determined from the lateral load transfer ratio shown in eq. (21).

Simulation Results

In order to show the effectiveness of the proposed tuning algorithm in the nonlinear bicycle model, two different vehicle maneuvers (ramp steer and sine-with-dwell) have been performed in the simulation.

For the ramp steer test, a steering input shown in Fig. 7 (steering rate is 40 deg/s) is applied while vehicle runs at 120 km/h. Figs. 14 and 15 illustrate comparison of vehicle trajectory and vehicle lateral acceleration with CarSim, nonlinear bicycle model, and the nonlinear bicycle model with proposed tuning algorithm, respectively. It can be seen that the trajectory of the nonlinear bicycle model with a proposed tuning algorithm is closely matched with Carsim. This is a significant improvement compared with the nonlinear bicycle model as shown in Fig. 14.

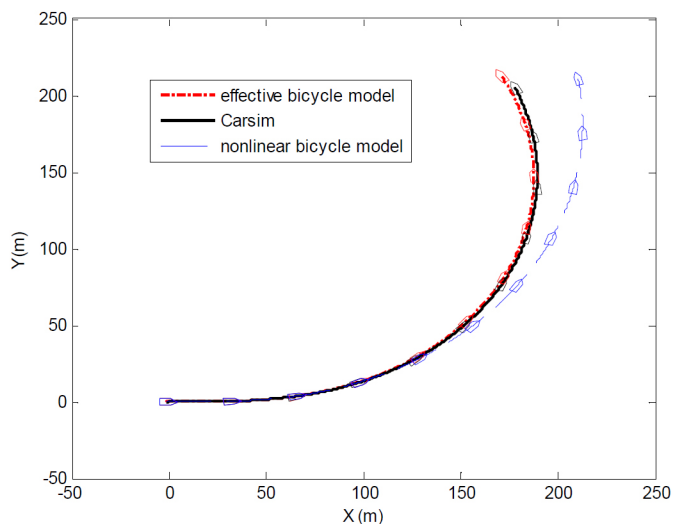


Fig. 14. Vehicle trajectory comparison for the ramp steer input at a speed of 120 km/h

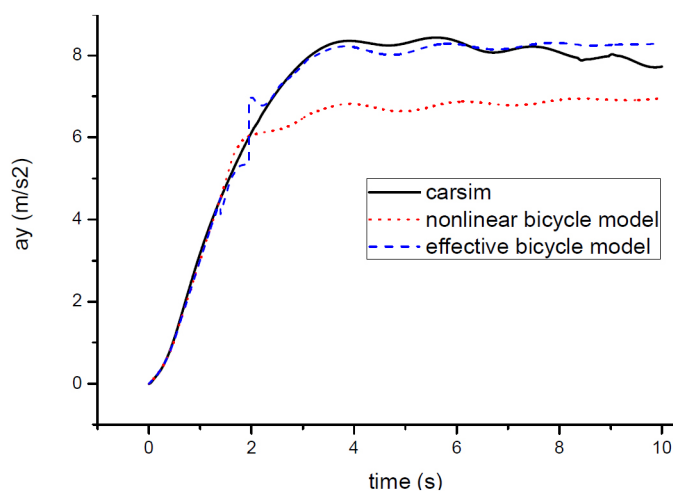


Fig. 15. Vehicle lateral acceleration comparison for the ramp steer input at a speed of 120 km/h

Fig. 15 compares lateral acceleration of three different vehicle models. It is observed that there is some notch phenomenon around 2 seconds in the effective bicycle model's result; this is caused by the tuning algorithm. It can be seen that with the proposed tuning algorithm, the lateral acceleration of a nonlinear bicycle model (effective bicycle model) is well matched with that of CarSim. However, the responses (trajectory and lateral acceleration) of a nonlinear bicycle model without the proposed tuning algorithm are quite different. This simulation result well demonstrates the effectiveness of the proposed tuning algorithm.

The sine-with-dwell maneuver is widely used to evaluate the performance of electronic stability control (ESC) system. In this section, the sine-with-dwell maneuver is performed for three different vehicle models and its responses are compared. Fig. 16 shows the steering wheel input of the sine-with-dwell maneuver where a vehicle runs at a constant vehicle speed of 100 km/h for the simulation.

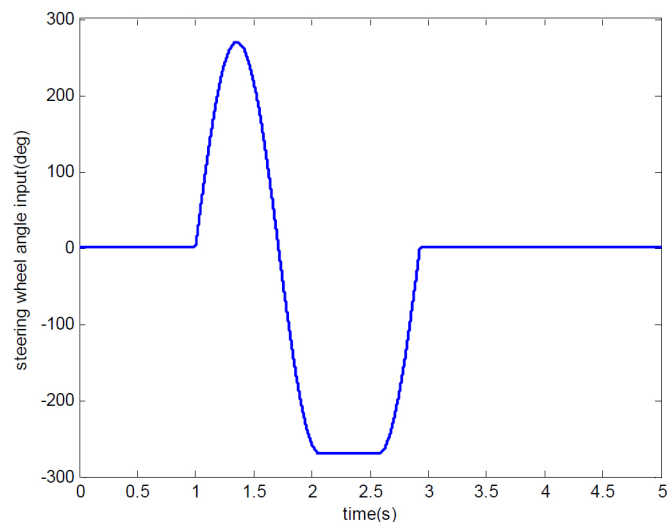


Fig. 16. Steering wheel input for a sine-with-dwell maneuver

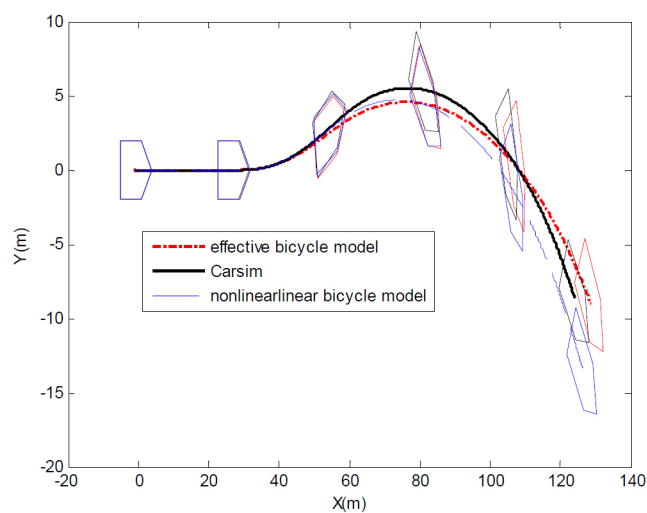


Fig. 17. Comparison of vehicle trajectory during a sine-with-dwell maneuver

Fig. 17 compares vehicle trajectories for three different vehicle models during the sine-with-dwell maneuver. As shown in this plot, the trajectory of the effective bicycle model (nonlinear bicycle model with the proposed tuning algorithm) is well matched with CarSim model. As indicated on Fig. 18, the lateral acceleration of the nonlinear bicycle model with parameter tuning is closely matched with that of CarSim.

From the above simulation results, it can clearly show the effectiveness of the proposed tuning method in the bicycle model. The vehicle trajectory of a bicycle model with the piecewise linear tire model and the proposed tuning algorithm is well matched with the trajectory of a CarSim for wide range of vehicle maneuvers. This model can be useful in the control system to generate realistic reference vehicle trajectory of a vehicle in the severe vehicle maneuvers.

It should be noted that although the simulation results show the good correlation with a CarSim in the plane motion, other vehicle responses are quite different and the proposed tuning method can be further improved.

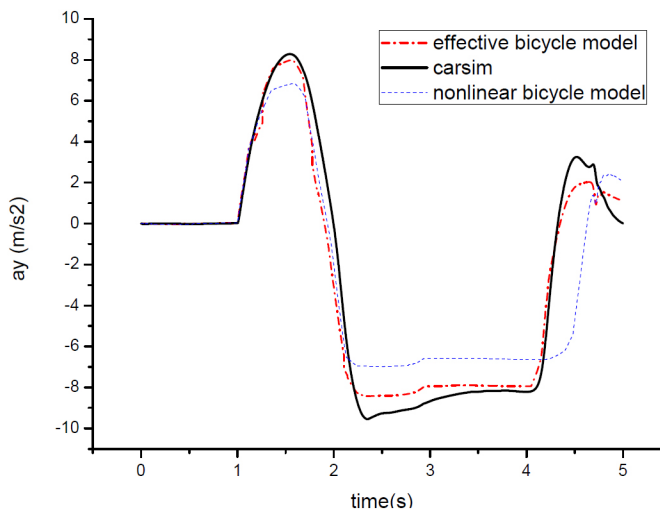


Fig. 18. Comparison of vehicle lateral acceleration during a sine-with-dwell maneuver

Conclusion

In this paper, vehicle responses of a bicycle model have been compared to the full car model. Vehicle trajectories of a bicycle model significantly deviate as vehicle operating condition changes and the tire force tuning algorithm has been proposed to improve the accuracy of bicycle model trajectory. Using a simplified piecewise linear tire model along with tire force tuning algorithm, the nonlinear bicycle model well follows a trajectory of the full car model. The proposed effective bicycle model can be used in the model predict control, state estimation algorithm or as reference in the controller design. In addition, it can also present a realistic and predictable behavior in some severe driving conditions such as collision avoidance maneuvers.

References

1. Oufroukh, N.A, Benine-Neto, et.al. (2011): Invariant set based vehicle handling improvement at tire saturation using fuzzy output feedback," Intelligent Vehicles Symposium (IV), 2011 IEEE, vol., no., pp.1104, 1109.
2. Chen Chih-Keng, Dao Trung-Kien. (2010): A Study of Bicycle Dynamics via System Identification. International Symposium on Computer, Communication, Control and Automation.
3. Westermarck C.. (2013): Validation of vehicle model in car simulator. Thesis. Royal Institute of technology, School of Engineering Sciences, Kungliga Tekniska Högskolan in Stockholm.
4. Ahn, Chang Sun. (2011): Robust Estimation of Road Friction Coefficient for Vehicle Active Safety Systems. Thesis, Mechanical Engineering in the University of Michigan.
5. Changfu Zong Heqi Liang Chengwei Tian Rufe Hu. Vehicle chassis coordinated control strategy based on model predictive control method. Information and Automation (ICIA), 2010 IEEE International Conference.
6. Yoshida Hidehisa, Shinohara Shuntaro & Nagai Masao (2008): Lane change steering manoeuvre using model predictive control theory, Vehicle System Dynamics: International Journal of Vehicle Mechanics and Mobility, 46:S1, 669-681, DOI:10.1080/00423110802033072.
7. Falcone Paolo, Tseng H. Eric, Borrelli Francesco, Asgari Jahan & Hrovat Davor (2008): MPC-based yaw and lateral stabilisation via active front steering and braking, Vehicle System Dynamics: International Journal of Vehicle Mechanics and Mobility, 46:S1, 611-628, DOI:10.1080/00423110802018297.
8. Doumiati M, Senane O, Dugard L, et al. (2013): Integrated vehicle dynamics control via coordination of active front steering and rear braking. European Journal of Control.
9. Hindiyeh RY, Gerdes JC. A controller framework for autonomous drifting: Design, stability, and experimental validation. Proceedings, 2011 ASME Dynamic Systems and Control Conference.
10. Canale M, Fagiano L, Milanese M, Borodani P (2007): Robust vehicle yaw control using a differential and IMC techniques. Control Engineering Practice; 15(8):923-941.
11. Pacejka, Besselink (1997): Magic Formula Tire Model with Transient Properties. Vehicle system dynamics, volume 27.
12. Guntur R. and Sankar (1980): A friction circle concept for Dugoff's tire friction model. Int. J. of Vehicle Design, Vol 1. No. 4.
13. Tsiotras P. et al. (2004): A LuGre Tire Friction Model with Exact Aggregate, Vehicle System Dynamics.
14. Guo, K. and Ren, L., "A Unified Semi-Empirical Tire Model with Higher Accuracy and Less Parameters," SAE Technical Paper 1999-01-0785, 1999, doi:10.4271/1999-01-0785.
15. Adireddy, G., Shim, T and Rhode, D., "Wheel Torque Controller Development Using a Simplified Tire Model for Vehicle Handling Enhancement," ASME 2009 Dynamics Systems and Control Conferences, Hollywood, CA, October 12-14, 2009.
16. Shim, T. Margolis, D., "An Analytical Tire Model for Vehicle Simulation in Normal Driving Condition," International Journal of Vehicle Design, Vol. 35, No. 3, 2004, pp.224-240.
17. Pacejka, H., "Tire and Vehicle Dynamics," Society of Automotive Engineers, Inc. and Butterworth Heinemann, Warrendale, PA, ISBN 978-0-7680-1126-5, 2002.
18. CarSim Website:<http://www.carsim.com>, Mechanical Simulation Corporation, 2008.

The Engineering Meetings Board has approved this paper for publication. It has successfully completed SAE's peer review process under the supervision of the session organizer. The process requires a minimum of three (3) reviews by industry experts.

All rights reserved. No part of this publication may be reproduced, stored in a retrieval system, or transmitted, in any form or by any means, electronic, mechanical, photocopying, recording, or otherwise, without the prior written permission of SAE International.

Positions and opinions advanced in this paper are those of the author(s) and not necessarily those of SAE International. The author is solely responsible for the content of the paper.